

# The space density of high-redshift QSOs in the GOODS Survey <sup>1</sup>

S.Cristiani<sup>1,8</sup>, D.M.Alexander<sup>2,10</sup>, F.Bauer<sup>2</sup>, W.N.Brandt<sup>2</sup>, E.T.Chatzichristou<sup>3</sup>,  
 F.Fontanot<sup>4</sup>, A.Grazian<sup>5</sup>, A.Koekemoer<sup>6</sup>, R.A.Lucas<sup>6</sup>, P.Monaco<sup>4</sup>, M.Nonino<sup>1</sup>,  
 P.Padovani<sup>6,9</sup>, D.Stern<sup>7</sup>, P.Tozzi<sup>1</sup>, E.Treister<sup>3</sup>, C.M.Urry<sup>3</sup>, E.Vanzella<sup>8</sup>

## ABSTRACT

We present a sample of 17 high-redshift ( $3.5 \lesssim z \lesssim 5.2$ ) QSO candidates in the 320 arcmin<sup>2</sup> area of the Great Observatories Origins Deep Survey, selected in the magnitude range  $22.45 < z_{850} < 25.25$  using deep imaging with the Advanced Camera for Surveys onboard the *Hubble Space Telescope* and the Advanced CCD Imaging Spectrometer onboard the *Chandra X-ray Observatory*. On the basis of seven spectroscopic and ten photometric redshifts we estimate that the final sample will contain between two and four QSOs with  $4 < z < 5.2$ . A dearth of high-redshift, moderate-luminosity ( $M_{145} \simeq -23$ ) QSOs is observed with respect to predictions based on *a*) the extrapolation of the  $z \sim 2.7$  luminosity function (LF), according to a pure luminosity evolution calibrated by the results of the Sloan Digital Sky Survey; and *b*) a constant universal efficiency in the formation of super-massive black holes (SMBHs) in dark-matter halos. Evidence is gathered in favor of a density evolution of the LF at high redshift and of a suppression of the formation or feeding of SMBHs in low-mass halos.

*Subject headings:* quasars: general; galaxies: active; cosmology: observations

---

<sup>1</sup>INAF-Osservatorio Astronomico, Via Tiepolo 11, I-34131 Trieste, Italy, e-mail: cristiani@ts.astro.it

<sup>2</sup>Department of Astronomy and Astrophysics, Pennsylvania State University, 525 Davey Lab, University Park, PA 16802

<sup>3</sup>Department of Astronomy, Yale University, PO Box 208101, New Haven, CT06520

<sup>4</sup>Dipartimento di Astronomia dell'Università, Via Tiepolo 11, I-34131 Trieste, Italy

<sup>5</sup>INAF-Osservatorio Astronomico di Roma, via Frascati 33, I-00040 Monteporzio, Italy

<sup>6</sup>Space Telescope Science Institute, 3700 San Martin Dr., Baltimore, MD 21218

<sup>7</sup>Jet Propulsion Laboratory, California Institute of Technology, Mail Stop 169-506, Pasadena, CA 91109

<sup>8</sup>European Southern Observatory, K.Schwarzschild-Straße 2, D-85748 Garching, Germany

<sup>9</sup>ESA Space Telescope Division

<sup>10</sup>Institute of Astronomy, Madingley Road, Cambridge, CB3 0HA, UK

## 1. Introduction

QSOs are intrinsically luminous and therefore can be seen rather easily at large distances; however, they are rare, and so finding them requires surveys over large areas. As a consequence, at present, the number density of QSOs at high redshift is not well known. Recently, the Sloan Digital Sky Survey (SDSS) has produced a breakthrough, discovering QSOs up to  $z = 6.43$  (Fan et al. 2003) and building a sample of six QSOs with  $z > 5.7$ . The SDSS, however, is sensitive only to very luminous QSOs ( $M_{145} \lesssim -26.5$ ) and provides no information about the faint end of the high- $z$  QSO LF, which is particularly important to understand the interplay between the formation of galaxies and super-massive black holes (SMBH) and to measure the QSO contribution to the UV ionizing background (Madau, Haardt & Rees 1999). New deep multi-wavelength surveys like the Great Observatories Origins Deep Survey (GOODS) provide significant constraints on the space density of less luminous QSOs at high redshift. Here we present high- $z$  QSO candidates, identified in the two GOODS fields on the basis of deep imaging in the optical (with *HST*) and X-ray (with *Chandra*), and discuss the allowed space density of QSOs in the early universe. We adopt a definition of QSOs comprising all objects with strong, high-ionization emission lines and  $M_{145} \leq -21$ , including both conventional, broad-lined (type-1) QSOs and narrow-lined, obscured (type-2) QSOs. Throughout this paper we use a cosmology with  $h, \Omega_{\text{tot}}, \Omega_m, \Omega_\Lambda = 0.7, 1.0, 0.3, 0.7$ ; magnitudes and colors are measured in the AB system.

## 2. The Database

The present work surveys an area of  $320 \text{ arcmin}^2$ , subdivided in two fields centered on the *Chandra* Deep Field-South (CDF-S) and Hubble Deep Field-North (HDF-N), each covering  $\approx 10' \times 16'$ . The optical data have been obtained with the Advanced Camera for Surveys (ACS) onboard *HST* in the framework of the GOODS/ACS survey described in Giavalisco et al. (2003a). Mosaics have been created from the first three epochs of observations, out of a total of five, in the bands F435W( $B_{435}$ ), F606W( $V_{606}$ ), F775W ( $i_{775}$ ), F850LP( $z_{850}$ ). The catalogs used to select high- $z$  QSOs have been generated using the SExtractor software, performing the detection in the  $z_{850}$  band and then using the isophotes defined during this process as apertures for photometry in the other bands (Giavalisco et al. 2003a).

The HDF-N and CDF-S fields have X-ray observations of 2 Ms and 1 Ms, respectively

---

<sup>1</sup>Based on observations taken with the NASA/ESA Hubble Space Telescope, which is operated by the Association of Universities for Research in Astronomy, Inc. (AURA) under NASA contract NAS5-26555.

(Alexander et al. 2003, hereafter A03; Giacconi et al. 2002, hereafter G02), providing the deepest views of the Universe in the 0.5–8.0 keV band. The X-ray completeness limits over  $\approx 90\%$  of the area of the GOODS fields are similar, with flux limits ( $S/N=5$ ) of  $\approx 1.7 \times 10^{-16}$  erg cm $^{-2}$  s $^{-1}$  (0.5–2.0 keV) and  $\approx 1.2 \times 10^{-15}$  erg cm $^{-2}$  s $^{-1}$  (2–8 keV) in the HDF-N field, and  $\approx 2.2 \times 10^{-16}$  erg cm $^{-2}$  s $^{-1}$  (0.5–2.0 keV) and  $\approx 1.5 \times 10^{-15}$  erg cm $^{-2}$  s $^{-1}$  (2–8 keV) in the CDF-S field (A03). The sensitivity at the aim point is about 2 and 4 times better for the CDF-S and HDF-N, respectively. As an example, assuming an X-ray spectral slope of  $\Gamma = 2.0$ , a source detected with a flux of  $1.0 \times 10^{-16}$  erg cm $^{-2}$  s $^{-1}$  would have both observed and rest-frame luminosities of  $8 \times 10^{42}$  erg s $^{-1}$ , and  $3 \times 10^{43}$  erg s $^{-1}$  at  $z = 3$ , and  $z = 5$ , respectively (assuming no Galactic absorption). A03 produced point-source catalogs for the HDF-N and CDF-S and G02 for the CDF-S.

### 3. Selection of the QSO candidates and determination of the redshifts

The selection of the QSO candidates has been carried out in the magnitude interval  $22.45 < z_{850} < 25.25$ . QSO colors in the ACS bands (Fig. 1) have been estimated as a function of redshift using a template (Cristiani & Vio 1990, CV90) of the QSO spectral energy distribution (SED) convolved with the Madau, Haardt & Rees (1999) model of the intergalactic medium (IGM) absorption. Four optical criteria have been tailored in order to select QSOs at progressively higher redshift in the interval  $3.5 \lesssim z \lesssim 5.2$ :

$$i - z < 0.35 \text{ AND } 1.1 < B - V < 3.0 \text{ AND } V - i < 1.0 \quad (1)$$

$$i - z < 0.35 \text{ AND } B - V > 3.0 \quad (2)$$

$$i - z < 0.5 \text{ AND } B - V > 2.0 \text{ AND } V - i > 0.8 \quad (3)$$

$$i - z < 1.0 \text{ AND } V - i > 1.9 \quad (4)$$

They select a broad range of high- $z$  AGN, not limited to broad-lined (type-1) QSOs, and are less stringent than those typically used to identify high- $z$  galaxies (e.g., Giavalisco et al. 2003b). Below  $z \simeq 3.5$  the typical QSO colors in the ACS bands move close to the locus of stars and low-redshift galaxies. Beyond  $z \simeq 5.2$  the  $i - z$  color starts increasing and infrared bands would be needed to identify QSOs efficiently with an “ $i$ -dropout” technique. To avoid contamination from spurious sources we have limited our selection to  $z_{850}$  detections with  $S/N > 5$ . The criteria have been applied independently and produced in total 645 candidates in the CDF-S and 557 in the HDF-N.

Two QSOs were found in the literature within the magnitude and redshift ranges of interest ( $22.45 < z_{850} < 25.25$ ,  $3.5 \leq z \leq 5.2$ ): CDF-S 033229.8 – 275105 ( $z = 3.700$ ) and

HDF-N 123647.9 + 620941 ( $z = 5.186$ ). Both have been selected with the present criteria <sup>12</sup>. Ten galaxies with  $3.5 \leq z \leq 5.2$  are known in the HDF-N (Cohen et al. 2000; Dawson et al. 2001, 2002). Eight are selected with the color criteria (1-4) (see Fig. 1). The two missed objects (HDF-N 1236279+6217504 and 1236376+621453) are both positionally uncertain identifications with a spectrum “solo-line with no continuum” (Dawson et al. 2001). HDF-N 1236279+6217504 has no optical counterpart in our ACS photometric catalog, and the supposed counterpart of HDF-N 1236376+621453 has colors very far from our criteria ( $B_{435} - V_{606} = 1.4$ ,  $i_{775} - z_{850} = 1.3$ ,  $V_{606} - i_{775} = 2.3$ ).

The optical candidates selected with the criteria (1-4) have been matched with X-ray sources detected by *Chandra* (A03, G02) within an error radius corresponding to the  $3 \sigma$  X-ray positional uncertainty. With this tolerance the expected number of false matches is five and indeed two misidentifications, i.e. cases in which a brighter optical source lies closer to the X-ray position, have been rejected (both in the CDF-S). The sample has been reduced in this way to 11 objects in the CDF-S and 6 in the HDF-N (Tab. 1). Type-1 QSOs with  $M_{145} < -21$ , given the measured dispersion in their optical-to-X-ray flux ratio (Vignali et al. 2003), should be detectable in our X-ray observation up to  $z \gtrsim 5.2$ . Conversely, any  $z > 3.5$  source in the GOODS region detected in the X-rays must harbor an AGN ( $L_x(0.5 - 2 \text{ keV}) \gtrsim 10^{43} \text{ erg s}^{-1}$ ).

Photometric redshifts of the 17 QSO candidates (Tab. 1, Col. 11) have been estimated by comparing with a  $\chi^2$  technique (see Arnouts et al. (1999) for details) the observed ACS colors to those expected on the basis of *a*) a library of template SEDs of galaxies (the “extended Coleman” of Arnouts et al. (1999)); *b*) the QSO SED described in § 3. In general the estimates *a*) and *b*) are similar, since the criteria (1-4) both for galaxies and QSOs rely on a strong flux decrement in the blue part of the spectrum - due to the IGM and possibly an intrinsic Lyman limit absorption - superimposed on an otherwise blue continuum. Seven objects out of the 17 selected have spectroscopic confirmations (Tab. 1, Col. 12). Four are QSOs with redshifts between 2.7 and 5.2, in good agreement with the photometric redshifts based on the QSO SED. Three are reported to be galaxies and the relatively large offsets between the X-ray and optical positions suggest that they could be misidentifications.

---

<sup>12</sup>The X-ray emitting radio galaxy HDF-N 123642.0 + 621331, identified by Waddington et al. (1999) at  $z = 4.424$ , has not been selected. It should be noted, however, that the redshift of this source has been questioned by Barger, Cowie & Richards (2000).

#### 4. Discussion and Conclusions

We have compared the QSO counts observed in the  $z_{850}$  band with two phenomenological and two more physically motivated models (Fig. 2). In the absence of a complete spectroscopic follow-up we focus the comparison in the redshift range  $4 \leq z \leq 5.2$ , where the selection criteria (1-4) and the photometric redshifts are expected to be highly complete and reliable. In addition to one spectroscopically confirmed QSO (HDF-N 123647.9 + 620941,  $z = 5.186$ ) we estimate that between 1 – 3 more QSOs at  $z > 4$  are present in the GOODS, depending on whether galaxy or QSO SEDs are adopted for the photometric redshifts.

*Phenomenological models.* The double power-law fit of the 2QZ QSO LF (Boyle et al. 2000) has been extrapolated for  $z > 2.7$  (the peak of QSO activity) in a way to produce a power-law decrease of the number of bright QSOs by a factor 3.5 per unit redshift interval, consistent with the  $3.0_{-0.9}^{+1.3}$  factor found by Fan et al. (2001). The extrapolation is carried out either as a Pure Luminosity Evolution (PLE) or a Pure Density Evolution (PDE), assuming that the slopes of the LF power-laws remain unchanged all the way up to  $z \sim 5$ . The PLE model predicts about 17 QSOs with  $z_{850} < 25.25$  at redshift  $z > 4$  (27 at  $z > 3.5$ ) in the 320 arcmin<sup>2</sup> of the two GOODS fields, and is inconsistent with the observations at a more than  $3\sigma$  level. The PDE estimate is 2.9 QSOs at  $z > 4$  (6.7 at  $z > 3.5$ ).

*Physically motivated models.* It is possible to connect QSOs with DMH formed in hierarchical cosmologies with a minimal set of assumptions (MIN model, e.g. Haiman & Hui (2001)): *a*) QSOs are hosted in newly formed halos with *b*) a constant SMBH/DMH mass ratio  $\epsilon$  and *c*) accretion at the Eddington rate. The bolometric LF of QSOs is then:

$$\Phi(L|z)dL = n_{\text{PS}}(M_H|z) \int_{t(z)-t_{\text{duty}}}^{t(z)} P(t_f|M_H, t(z))dt_f \epsilon^{-1} \frac{dL}{L_{\text{Edd}}} \quad (5)$$

where the abundance of DMHs of mass  $M_H$  is computed using the Press & Schechter (1974) recipe, the distribution  $P(t_f|M_H, t(z))dt_f$  of the formation times  $t_f$  follows Lacey & Cole (1993),  $t_{\text{duty}}$  is the QSO duty cycle and  $L_{\text{Edd}} = 10^{4.53} L_{\odot}$  is the Eddington luminosity of a  $1 M_{\odot}$  SMBH. The MIN model is known to overproduce the number of high- $z$  QSOs (Haiman, Madau & Loeb 1999) and in the present case predicts 151 QSOs at  $z > 4$  (189 at  $z > 3.5$ ). Alternatively, QSOs are assumed to shine a  $t_{\text{delay}}$  time after DMH formation (DEL model; Monaco, Salucci & Danese 2000; Granato et al. 2001). The QSO LF of eq. 5 is then computed at a redshift  $z'$  corresponding to  $t(z) - t_{\text{delay}}$ . The predictions of the DEL model are very close to the PDE, with 3.2 QSOs expected at  $z > 4$  (4.8 at  $z > 3.5$ ), in agreement with the observations. While all the models presented here are consistent with the recent QSO LF measurement of the COMBO-17 survey (Wolf et al. 2003) at  $z \simeq 2 - 3$ , only the PDE and DEL models fit the COMBO-17 LF in the range  $4.2 < z < 4.8$  and  $M_{145} < -26$ .

At  $z > 4$  the space density of moderate luminosity ( $M_{145} \simeq -23$ ) QSOs is significantly lower than the prediction of simple recipes matched to the SDSS data, such as a PLE evolution of the LF or a constant universal efficiency in the formation of SMBH in DMH. A similar result has been obtained at  $5 \lesssim z \lesssim 6.5$ , by Barger et al. (2003) who also showed that the QSO contribution to the UV background is insufficient to ionize the IGM at these redshifts. A flattening of the observed high- $z$  LF is required below the typical luminosity regime ( $M_{145} \lesssim -26.5$ ) probed by the SDSS. This is an indication that at these early epochs the formation or the feeding of SMBH is strongly suppressed in relatively low-mass DMH, as a consequence of feedback from star formation (Granato et al. 2001) and/or photoionization heating of the gas by the UV background (Haiman, Madau & Loeb 1999).

We are grateful to H.Spinrad, S.Dawson, and A.Dey for providing the redshift for HDF-N 123627.5+621158 and to C.Steidel for the spectrum of the galaxy HDF-N 123644.1+621311. The work of DS was carried out at the Jet Propulsion Laboratory, California Institute of Technology, under a contract with NASA. DMA, FEB, and WNB thank the NSF CAREER award AST-9983783. DMA also acknowledges the support provided by a Royal Society University Research Fellowship. We thank STScI grant HST-GO-09425.26-A (FEB, WNB), HST-GO-09425.13-A (CMU, EC, ET), and ASI grant I/R/088/02 (SC, AG, MN, EV).

## REFERENCES

- Alexander, D.M., et al. 2003, AJ 126, 539
- Arnouts, S., Cristiani, S., Moscardini, L., Matarrese, S., Lucchin, F., Fontana, A., Giallongo, E., 1999, MNRAS 310, 540
- Barger, A.J., Cowie, L.L., Richards, E.A., 2000, AJ 119, 2092
- Barger, A.J., Cowie, L.L., Bautz, M.W., Brandt, W.N., Garmire, G.P., Hornschemeier, A.E., Ivison, R.J, Owen, F.N., 2001, AJ 122, 2177
- Barger, A.J., Cowie, L.L., Brandt, W.N., Capak, P., Garmire, G.P., Hornschemeier, A.E., Steffen, A.T., Wehner, E.H., 2002, AJ 124, 1839
- Barger, A.J., Cowie, L.L., Capak, P., Alexander, D.M., Bauer, F.E., Brandt, W.N., Garmire, G.P., Hornschemeier, A.E., 2003, ApJ 584, L61
- Boyle, B.J., Shanks, T., Croom, S.M., Smith, R.J., Miller, L., Loaring, N., & Heymans, C., 2000, MNRAS 317, 1014

- Cohen, J.G., Hogg, D.W., Blandford, R., Cowie, L.L., Hu, E., Songaila, A., Shopbell, P., Richberg, K., 2000, ApJ 538, 29
- Cristiani, S., Vio R., 1990, A&A, 227, 385
- Cristiani, S., et al., 2000, A&A, 359, 489
- Dawson, S., Stern, D., Bunker, A.J., Spinrad, H., Dey, A., 2001, AJ 122, 598
- Dawson, S., Spinrad, H., Stern, D., Dey, A., van Breugel, W., de Vries, W., Reuland, M., 2002, ApJ 570, 92
- Dickinson, M., 1998, in *The Hubble Deep Field*, ed. M. Livio, S. M. Fall, P. Madau (Cambridge: Cambridge Univ. Press), 219
- Fan, X., et al., 2001, AJ 121,54
- Fan, X., Strauss, M.A., Schneider, D.P., Becker, R.H., AJ 125, 1649
- Giacconi, R., et al. 2002, ApJS, 139, 369, G02
- Giavalisco et al. 2003a, this volume
- Giavalisco et al. 2003b, this volume
- Granato, G.L., Silva, L., Monaco, P., Panuzzo, P., Salucci, P., De Zotti, G., Danese, L., 2001, MNRAS 324, 757
- Haiman, Z., & Hui, L., 2001, ApJ 547, 27
- Haiman, Z., Madau, P., & Loeb, A., 1999, ApJ 514, 535
- Lacey, C., & Cole, S., 1993, MNRAS 262, 627
- Madau, P., Haardt, F., Rees, M.J., 1999, ApJ 514, 648
- Monaco, P., Salucci, P., Danese, L., 2000, MNRAS 311, 279
- Norman, C., et al. 2002, ApJ 571, 218
- Press, W.H., & Schechter, P., 1974, ApJ 187, 425
- Schmitt, H.R., Kinney, A.L., Calzetti, D., Storchi-Bergmann, T., 1997, AJ 114, 592
- Vignali, C., et al. 2003, AJ 125, 2876

Waddington, I., Windhorst, R.A., Cohen, S.H., Partridge, R.B., Spinrad, H., Stern, D., 1999, *ApJ* 526, L77

Wolf, C., Wisotzki, L., Borch, A., Dye, S., Kleinheinrich, M., Meisenheimer, K., 2003, *astro-ph/0304072*

Table 1. High-redshift QSO candidates in the CDF-S.

| Optical     |                    | Optical – X-ray |              | $z_{850}$ | $B - V$ | $i - z$ | $V - i$ | $F_x$ ¶                                 | $F_x$ ¶                                 | phot.      | spectr.            |
|-------------|--------------------|-----------------|--------------|-----------|---------|---------|---------|---|---|------------|--------------------|
| RA          | DEC                | $\Delta$ RA     | $\Delta$ DEC | AB        | AB      | AB      | AB      | 0.5 – 2 keV                             | 2 – 8 keV                               | redshift   | redshift           |
| $3^h + m s$ | $-27^\circ + ' ''$ | (arcsec)        | (arcsec)     | (mag)     | (mag)   | (mag)   | (mag)   | ( $10^{-16}$ erg s $^{-1}$ cm $^{-2}$ ) | ( $10^{-16}$ erg s $^{-1}$ cm $^{-2}$ ) | gal, QSO § |                    |
| 32 03.03    | 44 50.1            | +0.0            | +0.5         | 24.77     | 1.39    | 0.35    | 0.74    | 6.84                                    | 8.99                                    | 2.5,3.3    |                    |
| 32 04.94†   | 44 31.7            | +1.7            | –0.5         | 23.65     | 2.01    | 0.03    | 0.20    | < 0.74                                  | 4.10                                    | 3.7,3.7    | 3.462 <sup>a</sup> |
| 32 14.44    | 44 56.6            | –0.5            | –0.3         | 23.05     | 2.12    | 0.44    | 1.46    | 0.41                                    | < 4.3                                   | 0.7,4.3    |                    |
| 32 18.82    | 51 35.3            | –0.9            | +0.1         | 24.82     | 2.52    | 0.35    | 0.49    | 0.74                                    | 14.0                                    | 3.9,3.8    |                    |
| 32 19.40†   | 47 28.3            | +0.8            | –0.7         | 24.60     | 1.30    | 0.07    | 0.45    | < 0.31                                  | 1.17                                    | 3.4,3.5    |                    |
| 32 29.29‡   | 56 19.3            | –1.0            | +0.1         | 25.05     | > 3     | 0.12    | 1.65    | 0.50                                    | < 7.6                                   | 4.6,4.7    |                    |
| 32 29.85    | 51 05.8            | –0.1            | +0.1         | 24.59     | 2.25    | 0.01    | 0.59    | 3.06                                    | 31.8                                    | 3.7,3.8    | 3.700 <sup>b</sup> |
| 32 39.67    | 48 50.6            | –0.1            | +0.1         | 24.55     | 2.96    | 0.24    | 0.97    | 7.48                                    | 70.6                                    | 3.9,4.0    |                    |
| 32 41.87    | 52 02.5            | –0.3            | +0.1         | 22.47     | 1.24    | 0.22    | 0.46    | 16.7                                    | 38.2                                    | 0.5,3.6    |                    |
| 32 42.84    | 47 02.5            | +0.0            | –0.1         | 24.91     | 1.28    | 0.10    | –0.04   | 6.31                                    | 16.4                                    | 3.5,3.4    |                    |
| 32 50.25    | 52 51.9            | +0.3            | –0.2         | 25.19     | 1.54    | 0.10    | 0.32    | 24.0                                    | 75.3                                    | 0.6,3.6    |                    |

High-redshift QSO candidates in the HDF-N.

| $12^h + m s$ | $62^\circ + ' ''$ |      |      |       |      |       |      |        |       |         |                    |
|--------------|-------------------|------|------|-------|------|-------|------|--------|-------|---------|--------------------|
| 36 27.59     | 11 58.7           | –1.1 | +0.3 | 23.60 | 1.28 | 0.20  | 0.69 | 1.06   | 22.0  | 0.4,3.7 | 0.395 <sup>c</sup> |
| 36 42.21     | 17 11.6           | –0.1 | +0.1 | 24.01 | 1.12 | 0.22  | 0.59 | 9.48   | 23.2  | 2.8,2.9 | 2.724 <sup>d</sup> |
| 36 43.09     | 11 08.9           | –0.1 | +0.9 | 23.13 | 1.15 | –0.04 | 0.54 | 0.75   | < 2.0 | 0.4,3.5 | 0.299 <sup>e</sup> |
| 36 44.10†    | 13 11.0           | +0.1 | –1.1 | 23.87 | 1.35 | 0.06  | 0.45 | < 0.26 | < 1.4 | 3.4,3.6 | 2.929 <sup>f</sup> |
| 36 46.07     | 14 49.2           | +0.1 | +0.3 | 25.16 | 1.36 | 0.25  | 0.99 | < 0.34 | < 1.4 | 0.6,3.8 |                    |
| 36 47.96     | 09 41.6           | +0.1 | +0.3 | 23.72 | 4.45 | 0.13  | 2.12 | 2.72   | 4.89  | 4.7,4.8 | 5.186 <sup>g</sup> |

¶ Objects with upper limits both in the soft and hard band have been detected in other sub-bands.

§ The first photometric redshift is computed on the basis of galaxy SEDs, the second for QSO SEDs.

† From the supplementary X-ray catalog by A03.

‡ Detected in the X-ray by G02 and not by A03. X-ray coordinates and fluxes derived from G02. Positions in G02 are typically offset  $+0.07''$  in RA and  $-1''$  in DEC with respect to the optical ACS positions. The correction has been applied in Cols.3-4.

<sup>a</sup> QSO showing relatively narrow emission lines with a P-Cyg profile (Cristiani et al. 2000).

<sup>b</sup> Type-2 QSO (Norman et al. 2002).

<sup>c</sup> Galaxy: H. Spinrad, private communication.

<sup>d</sup> Broad emission-line QSO (Barger et al. 2001).

<sup>e</sup> Galaxy identified by Cohen et al. (2000).

<sup>f</sup> Galaxy identified by Dickinson (1998). No spectroscopic evidence for AGN activity is present in the spectrum.

<sup>g</sup> QSO identified by Barger et al. (2002).

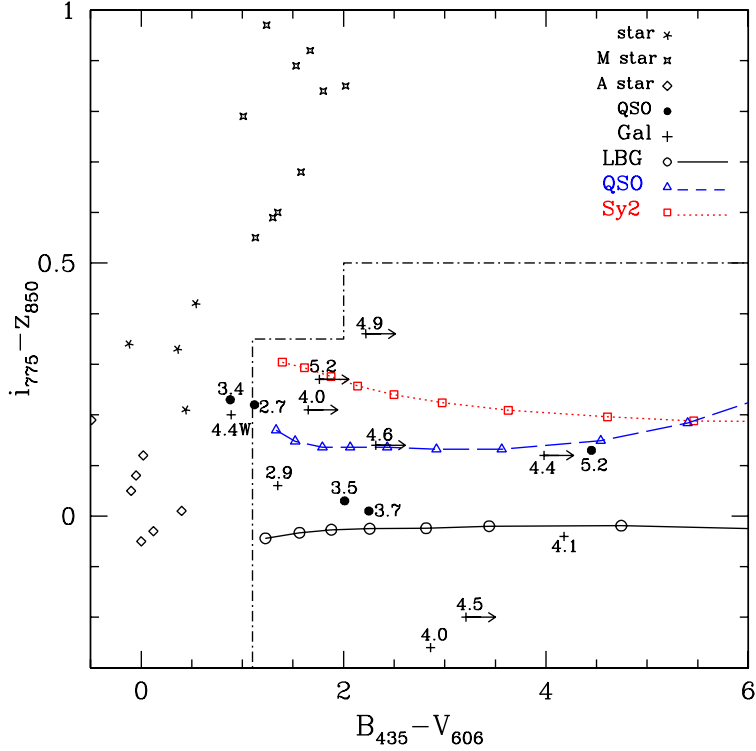


Fig. 1.— Expected  $i_{775} - z_{850}$  vs.  $B_{435} - V_{606}$  colors of QSOs as a function of redshift compared to other classes of objects. The dashed line shows the locus of QSOs at  $z \geq 3.5$  estimated with the composite spectrum of CV90. The continuous and dotted lines show the colors of Ly-break and Sy 2 galaxies, derived from the SEDs of Schmitt et al. (1997) and Arnouts et al. (1999), respectively. The corresponding symbols - open triangles, circles and squares - start on the left at  $z = 3.5$  and move to the right in steps of  $\Delta z = 0.1$ . The observed colors of five QSOs are marked with filled circles and the corresponding redshifts. The same is done for ten high- $z$  galaxies identified with crosses. The radio galaxy HDF-N 123642.0 + 621331 is marked with the label 4.4W. The positions of various types of stars is also shown. The dot-dashed line represents the projection of the selection criteria 1) + 3).

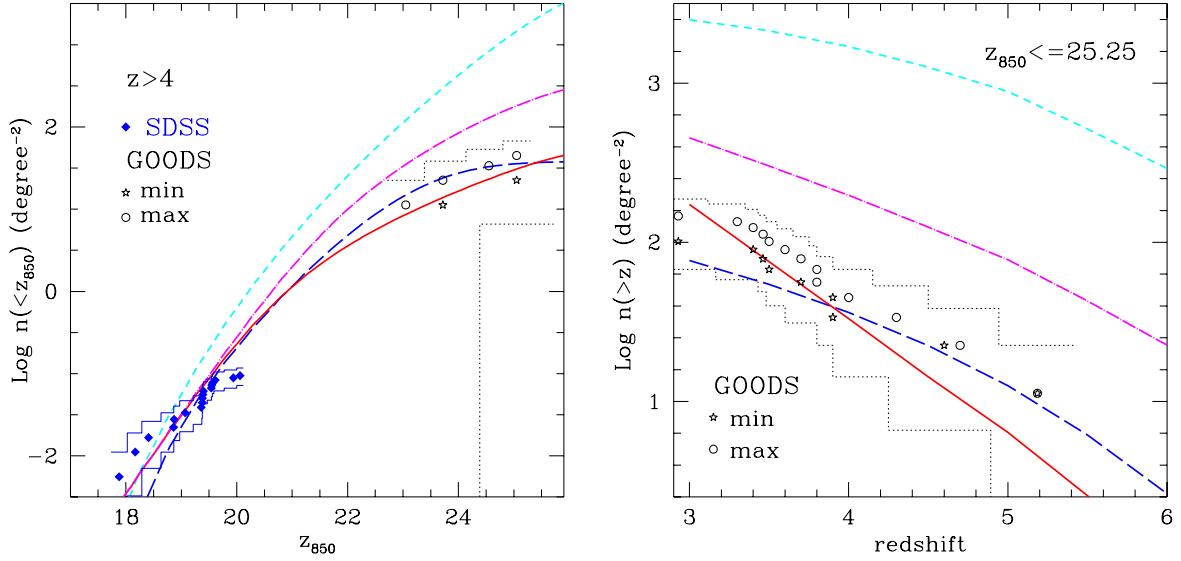


Fig. 2.— Comparison of the observed QSO counts and redshift distribution with model predictions. Circles and stars show the “maximal” and “minimal” estimates of the GOODS counts, respectively (see text). The dotted segments show the corresponding  $1\sigma$  upper (maximal case) and lower (minimal case) confidence limits. Models are represented by four smooth lines: dot-dashed PLE, continuous PDE, short-dash MIN (Haiman & Hui 2001), long-dash delayed QSO shining. A value of  $\sigma_8 = 0.83$  has been assumed in the MIN and DEL models, whose parameters have been fixed in order to reproduce the QSO LF at  $z \sim 3$ . In the MIN model:  $\log \epsilon = -3.2$  and  $t_{\text{duty}} = 0.015$  Gyr. In the DEL model:  $\log \epsilon = -3$  and  $t_{\text{duty}} = 0.013$  Gyr; the delay time  $t_{\text{delay}}(M_H)$  is set to 0.75 Gyr above  $10^{12.5} M_\odot$  and is decreased as  $\propto M_H^{-0.7}$  at lower masses (Granato et al. 2001). As dynamical and cooling times are shorter at high redshift,  $t_{\text{delay}}$  is assumed to decrease as  $(1+z)^{-2}$  above  $z = 2.7$ .